RADIATION COMPLEX ON THE BASIS OF HELIUM IONS LINAC

S.N. Dubniuk*, R.A. Anokhin, A.F. Dyachenko, A.P. Kobets, A.I. Kravchenko, O.V. Manuilenko, K.V. Pavlii, V.N. Reshetnikov, A.S. Shevchenko, V.A. Soshenko, S.S. Tishkin, B.V. Zajtsev, A.V. Zhuravlyov, V.G. Zhuravlyov
National Science Center "Kharkov Institute of Physics and Technology", Kharkov, Ukraine
****E-mail: sergdubnyuk@gmail.com***

The numerical simulation results and experimental investigation of helium ions linear accelerator with output energy 4 MeV and focusing by an RF field are presented. The variant of alternating-phase focusing with a step change in the synchronous phase and increasing amplitude of the RF field in accelerating gaps in the grouping section of the accelerating-focusing tract of the accelerator is used to ensure the radial-phase stability of the accelerated beam. The methods for increasing the accelerated ion beam current, as well as the beam current density on the target, are considered.

PACS: 29.17.w, 29.27.Bd

INTRODUCTION

Ion beams are widely used in science and industry: from high-energy and nuclear physics, plasma physics with magnetic and inertial confinement fusion, material science and medicine to ion beam-assisted deposition, implantation and track membranes production [1 - 10].

The critical issue in fusion reactors design, as well as nuclear power plants, is the influence of radiation on structural materials [11 - 14]. The irradiation of structural materials on ion accelerators makes it possible to study their behavior faster than in experimental nuclear reactors due to higher damage degree.

To study the structural materials behavior under the action of ionizing radiation, a radiation complex based on a helium ions linac was constructed. The radiation complex consists of the helium ions linear accelerator, the beam transporting and focusing system on a sample, the irradiation chamber for samples, the systems for *in-situ* measuring and controlling irradiation parameters in experiments.

The main elements of the ions linear accelerator are an injector (Fig. 1) and a resonator with an accelerating structure, placed in a vacuum chamber (Fig. 2). A special feature of the accelerator is the use of an alternating-phase focusing with a step-by-step change in the synchronous phase and an increasing amplitude of the RF field in accelerating gaps on the grouping part of the accelerating-focusing tract [15 - 17]. The linac injection energy and injection current are 120 keV and up to 10 mA, respectively, output energy is 4 MeV, and output current is 1 mA. Fig. 3 shows the beam transporting and focusing line from the output of the accelerating section to the irradiation chamber with samples.

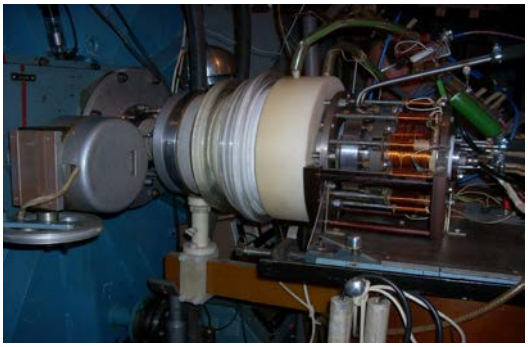

Fig. 1. Injector of the helium ions linac with an output energy of 120 keV

The paper present the injector, the accelerating structure and the beam transporting and focusing line on the target, as well as the results of numerical and experimental studies of beam dynamics in the accelerator and in the transport line in order to increase the beam current at the accelerator output and the beam current density on the target.

Fig. 2. Helium ions linac with an output energy of 4 MeV (foreground). Main section of the multicharged ions linac (background)

Fig. 3. Transport line for the helium ions beam. Left to right: irradiation chamber with samples, focusing triplet, output of the accelerator

1. HELIUM IONS INJECTOR

Helium ions injector was developed on the basis of a proton source to obtain helium ions with an energy of 30 keV/nucl. at the input of accelerator (Fig. 4) [18].

When a voltage pulse is applied to the anode, the discharge is ignited between the filament cathode (1) and the intermediate electrode (2). The plasma is drawn out to the anode (3) and anticathode (4) through the channel in the intermediate electrode. Magnetic fields of

the electromagnet (5) and the auxiliary coils (6) compresse plasma in the region between the intermediate electrode and the anticathode and increases the plasma density. Electrons oscillate in the potential well between the intermediate electrode and the anticathode, ionizing the neutral gas fed through the tube (9) into the cathode discharge region. The cathode part of the source, the intermediate electrode and the anode are cooled by water (7, 8, 10).

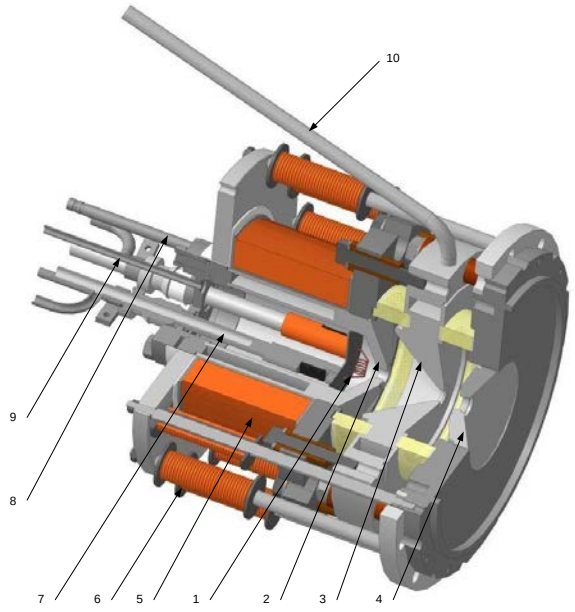

Fig. 4. Helium ions source

Fig. 5 shows the helium ions injector.

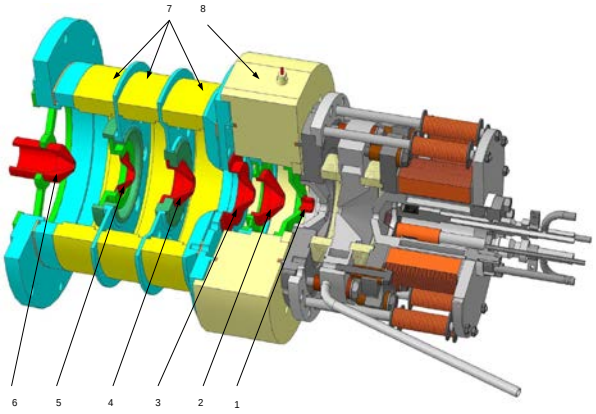

Fig. 5. Helium ions injector

It consists of an ion source (see Fig. 4) and a system of electrodes for extraction, focusing and acceleration a helium ions beam to energy of 120 keV. The voltage of 120 kV from the high-voltage modulator is supplied to the water based divider and distributed over the electrode system. The extraction (1) and focusing (2) electrodes are housed in a caprolon case (8). These electrodes are used for ions extraction from the plasma, and for beam formation, which is further accelerated by the accelerating tube (electrodes 3-6).

Between the accelerating tube electrodes there are ceramic rings (7) with a developed lateral surface, which withstand a potential difference up to 80 kV. This suppresses high-voltage breakdowns along the lateral surface. The stabilized supply voltage of the high-voltage modulator makes it possible to obtain at the accelerator input a helium ions beam with an energy up to 130 keV, up to 20 mA current and a minimum energy spread, which ensures an acceptable capture of the beam by the accelerating structure. The main parameters of the injector are given in Table 1.

Table 1

The main injector parameters

Working gas	helium
Arc current, A	2…6
Beam current at the output, mA	up to 20
Beam energy at the output, keV	up to 130
Beam diameter at the output, mm	~ 14
Working gas pressure in the source anode region, mmHg	$5 \cdot 10^{-3}$
Frequency of pulses, Hz	2…5
Arc modulator pulse width, μs	500
Magnetic field in source, oersted	300…1000
High-voltage modulator pulse width, μs	500

2. HELIUM IONS LINAC ACCELERATING STRUCTURE

When developing a helium ions linac, it was necessary to use existing production areas, existing equipment and technological infrastructure. At present, most linear accelerators in the range of small and medium energies are constructed according to the following scheme: (1) an ion source with an output energy of 50…120 keV, (2) a beam transport and matching system with the RFQ structure input, (3) an accelerating structure with RFQ, energy range 0.1…3 MeV, (4) structure with drift tubes and focusing elements arranged in them in the form of electromagnetic or solid quadrupole lenses.

Computer simulation has shown that in our case this approach is unacceptable. The acceleration rate in structures with RFQ is low, which leads to a significant elongation and the inability to place the structure in the available areas. Decreasing the length of the accelerating section by combining RFQ and the structure with drift tubes with electromagnetic lenses is difficult to realize because of the low particles velocity and the short drift tubes in which quadrupole lenses are to be placed.

An alternative option to ensure radial and longitudinal stability of the particle beam motion during acceleration is alternative-phase focusing (APF) [19]. In the APF, simultaneous radial and phase stability of the beam is achieved due to alternation of regions with negative and positive values of the synchronous phase. In this case, the longitudinal and transverse forces acting on the particle are of an alternating nature. Under certain conditions in such a system, it is possible to provide simultaneous longitudinal and phase stability of the particles beam motion during the acceleration process. The number of accelerating gaps in the focusing period can be different. With increasing particle energy, the total number of gaps entering the focusing period increases. This is due to the fact that focusing (or defocusing with a negative value of the synchronous phase) properties of the gap decrease in proportion to the particles velocity.

Therefore, in the APF the concept of "focusing period" is not entirely correct, since there is no periodicity. For each subsequent energy interval, we have to design our own "focusing period". The task is complicated by the fact that the focusing periods must be consistent with each other, taking into account the essential nonlinearity of particle dynamics. The nonlinearity of the particles dynamics in the APF is related not only to the nonlinearity of the Coulomb repulsion forces, but also to the connection of longitudinal and transverse motion. Particularly difficult for numerical simulation is the initial section of the accelerating-focusing channel with APF, on this site, in addition to the particles acceleration, there is the task of forming a bunch. In addition, the space charge forces in the accelerator initial part render the maximum influence on the beam dynamics.

Taking into account the foregoing, in order to ensure the required acceleration rate, with the maximum value of the particles capture coefficient in the acceleration regime, the number of accelerating-focusing periods, the phase distribution of the synchronous particle, and the magnitude of the RF field amplitude in the gaps are chosen as follows (Table 2):

Table 2

The linac accelerating-focusing channel structure

Period	The synchronous phase, degrees	Electric field, kV/cm
1	-90; 75; 60; 0; -60	27.5…37.5
2	-90; 75; 60; 0; -50	40…50
3	-85; 75; 60; 0; -65	52.5…62.5
4	-70; 75; 60; 0; -60	65…75
5	-70; 75; 60; 0; -60	75
6	-90; 75; 60; 40; 0; -60	75
7	-60	32.5

Table 2 shows that the accelerator consists of 6 focusing periods and one phasing accelerating gap. Each focusing period contains accelerating gaps with large absolute values of the synchronous phase, which ensure maximum capture of particles in the acceleration mode, and a gap with a zero synchronous phase, which has the maximum acceleration rate. To compensate for the decrease in the rigidity of focusing with increasing particle energy, acceleration gaps with an increasing amplitude of the rf field are used in the grouping region. The grouping section consists of four focusing periods, where the amplitude of the RF field increases from 27.5 to 75 kV/cm, by 2.5 kV/cm at each gap.

The accelerating channel calculation, taking into account the electrodes real configuration and the space charge forces, was carried out using the code APFRFQ [20]. Table 3 shows the main parameters.

The coefficient of beam capture into the acceleration mode is: for a beam current of 0 mA – 42%, for a beam current of 20 mA – 40%, for a current of 30 mA – 30%, which is not inferior to the accelerator [21] with APF, in which, as an accelerating-grouping area uses a structure with RFQ.

As an accelerating section for this channel, an H-resonator with drift tubes is used. The drift tubes in the resonator are fixed on its axis by means of rods, which facilitates the formation of a π-wave of the electric field along the accelerating section.

Table 3

Calculated parameters of the accelerating-focusing channel

Operating frequency, MHz	47.2
Injection energy, keV/nucleon	30
Output energy, MeV/nucleon	0.975
Accelerating cells number	32
Overall length, cm	237.7
Electric field strength in accelerating gaps, kV/cm	25…75
The maximum value of the electric field strength at accelerating electrodes, kV/cm	170
Aperture radius, cm	0.75…1.5
Input transverse beam emittance, mm·mrad	0.6
Accelerated current at injection current: 10 mA 20 mA 30 mA	 4 8 10

The length of the accelerating period is equal to $\beta\lambda/2$, where $\beta = v/c$ (v is the velocity of helium ions, c is the velocity of light, and λ is the wavelength of the electromagnetic field). In the considered region of the helium ion velocities, the H structures have a maximum shunt impedance ($R_{sh} \geq 50$ MΩ/m), which allows to significantly reduce the RF power. At the same time, the diameter of the resonator decreases considerably (approximately 4 times as compared with the E-cavity), which simplifies its manufacturing and placement in a vacuum casing (Fig. 6). The tuning of the structure was carried out by the methods given in [22 - 24].

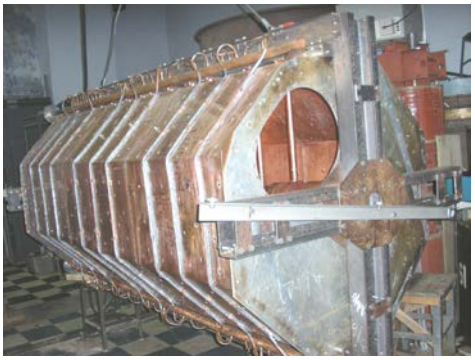

Fig. 6. Resonator view after the final technological assembly

Tuned acceleration section, manufactured according to the results of numerical calculations, differed slightly from the calculated one by its electrodynamic parameters (resonance frequency, acceleration field distribution along the structure gaps, Q-factor). Therefore, numerical simulation of the beam dynamics using the experimentally obtained electrodynamic parameters of the accelerating structure was carried out. The following results were obtained: at the injection current 3 mA, the accelerated current was 1 mA; at the injection current of 20…4.5 mA; at the injection current of 30…6 mA. Optimizing the operation of the injector, increasing the injector beam current, falling into the accelerator channel acceptance, led to an increase in the helium ions

accelerated current from 0.3 mA (initially) to 1 mA (now). Computer simulations show, the beam current can be increased to 4…5 mA with better matching of the beam emittance at the accelerator input and the acceleration channel acceptance.

Since the beam radius at the accelerating structure output is about 1.5 cm, it is possible to increase the beam current density of accelerated helium ions directly on the irradiating sample, using magnetic focusing at beam transporting to the target.

3. BEAM TRANSPORTING LINE

The channel for focusing and transporting the helium ion beam between the accelerating structure output and the sample irradiation chamber is designed to create the maximum current density of the accelerated beam on the target. For this purpose, a quadrupole focusing triplet is used with independent power supplies of the electromagnetic quadrupole lenses included in its composition. The triplet makes it possible to change the beam radius on the target, depending on the experimental requirements. As the accelerating structure constructed on the basis of the APF has an axisymmetric beam at the output, the most suitable is the use of a symmetric triplet. A symmetrical triplet consists of three electromagnetic quadrupole lenses with alternating focusing and defocusing actions. The first and last triplet lenses are of the same length. The middle lens length is the sum of the first and last lenses lengths. To calculate the transport channel with a focusing triplet and the particles dynamics in it, the output beam characteristics of the structure with APF were obtained using the APFRFQ code (Fig. 7): beam energy 4 MeV, beam current 4 mA, beam diameter 30 mm, the beam envelope inclination angle is 0 mrad. As a result of calculation and optimization of the triplet main parameters, the transport channel geometry, the magnetic field gradients magnitudes in the quadrupole lenses and the ions dynamics in the channel were obtained. The calculations were done taking into account the available equipment and the free space availability in the accelerator hall. Fig. 8 shows beam envelopes and the transportation line geometry. The numbers denote drift gaps: 1 – 347.5 mm, 3 – 75 mm, 5 – 70 mm, 7 – 297.5 mm; quadrupole magnetic lenses: 2 – 90 mm, 4 – 180 mm, 6 – 90 mm. The magnetic field gradients in the magnetic lenses centers: 2 – 18 T/m, 4 – 15.7 T/m, 6 – 18 T/m.

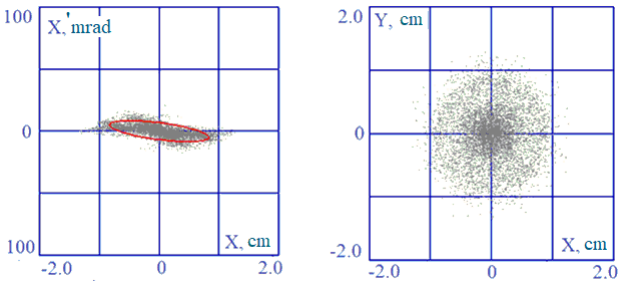

Fig. 7. Calculated values of the helium ion beam parameters at the accelerator output: transverse beam emittance (left); transverse beam geometric dimensions (right)

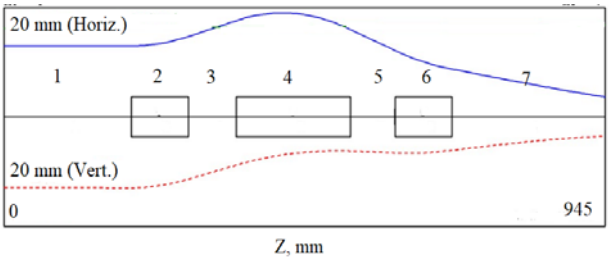

Fig. 8. Transport channel for the helium ion beam between the output of the accelerating structure and the sample irradiation chamber

Table 4 shows the measurements results of the magnetic field at various radial distances from the center for the triplet shown in Fig. 3. It is clear that the required magnetic field gradients at the magnetic lenses centers 18 and 15.7 T/m, can be obtained.

Table 4

Magnetic field vs current in the triplet lenses

Long lens					
4.5 mm		12.5 mm		20.5 mm	
I, A	B, T	I, A	B, T	I, A	B, T
1.0	0.012	1.0	0.043	1.0	0.077
2.0	0.022	2.0	0.083	2.0	0.148
3.0	0.032	3.0	0.123	3.0	0.215
4.0	0.043	4.0	0.158	4.0	0.283
5.0	0.049	5.0	0.188	5.0	0.337
6.0	0.055	6.0	0.209	6.0	0.375
6.4	0.057	6.55	0.217	6.55	0.389
Short lens					
4.5 mm		12.5 mm		20.5 mm	
I, A	B, T	I, A	B, T	I, A	B, T
1.0	0.016	1.0	0.043	1.0	0.062
2.0	0.028	2.0	0.079	2.0	0.124
3.0	0.04	3.0	0.114	3.0	0.186
4.0	0.051	4.0	0.142	4.0	0.239
5.0	0.058	5.0	0.163	5.0	0.277
6.0	0.064	6.0	0.179	6.0	0.302
7.0	0.068	7.0	0.192	7.0	0.325
8.0	0.072	8.0	0.202	8.0	0.342
9.0	0.075	9.0	0.210	9.0	0.356
10.0	0.078	10.0	0.218	10.0	0.369
10.35	0.079	10.1	0.218	10.7	0.378

The triplet is located between the output of the linac and the chamber for irradiating the samples. Investigations of the triplet focusing properties for a helium ions beam with an energy of 120 keV showed that if the current at the input to the triplet is 1.5 mA and at the output 0.7 mA, then after its switching on and tuning (the lenses currents are selected to obtain the maximum ion beam current at the output), the output current is equal to 1.25 mA. The ion beam current was measured with the help of flight sensors located at the accelerating structure output (in front of the triplet) and at the triplet output. Experiments with the 4 MeV beam indicated that a helium ions beam current (up to 0.8 mA) can be focused on a target in a spot about 1 cm in diameter.

Fig. 9 shows the focusing system adjustment equipment.

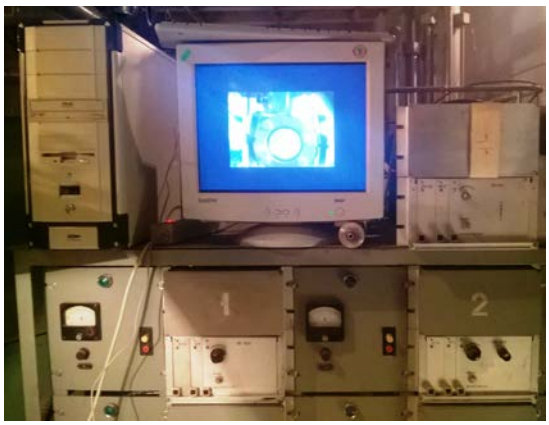

Fig. 9. The focusing system adjustment stand. The display shows the image of the output beam on the phosphor

CONCLUSIONS

The basic systems optimization of the helium ions linac with an output energy 4 MeV made it possible to increase the accelerated beam current up to 1 mA. Computer simulation of the beam dynamics in the accelerator performed for the experimentally obtained distributions of the RF field amplitude along the accelerating structure, shows that the current of the accelerated helium ion beam can be increased to 4…5 mA. For this, it is necessary to improve the matching of the beam emittance at the accelerator input with the acceleration channel acceptance.

The system for transporting and focusing the beam on the target was calculated, fabricated and mounted. It reduces beam losses during its transport to the target and focuses the beam on the sample into a spot of diameter about 1 cm. Experiments with a beam with an energy 120 keV showed that if the current at the input to the triplet is 1.5 mA and at the output 0.7 mA, then after switching on and setting the triplet, the current at its output is 1.25 mA. Preliminary experiments with a beam (an energy of 4 MeV) indicated that a helium ions beam current (up to 0.8 mA) can be produced on the target in a spot about 1 cm in diameter.

Numerical estimates made using the SRIM code, for a beam of 4 MeV helium ions, a pulse current 780 μA, a current pulse duration of 500 μs, a repetition rate of 5 pulses per sec and 1 cm in diameter on the target, for tungsten give 0.25 dpa/hour, and for iron – 0.14 dpa/hour.

The helium ion accelerator (A/q = 4, ion energy at the output of 0.975 MeV/nucl.) can be used as an injector for the multicharged ions accelerator main section (A/q = 5, injection energy is 0.975 MeV/nucl., output energy is 8.5 MeV/nucl., see Fig. 2). Currently, as an injector for the multicharged ions accelerator main section, an ion accelerator consisting of RFQ [25] and a structure with combined high-frequency focusing [16, 26, 27] is also being developed. This will increase the accelerated current to 10 mA, reduce the injection energy from 33 to 6 keV/nucl., expand the range of accelerated ions to A/q ≤ 20, to carry out experimental studies on the merger of heavy nuclei [28, 29].

REFERENCES

1. V.A. Bomko, A.M. Yegorov, B.V. Zaytsev, et al. Development of the MILAC complex for nuclear physical investigations // *Problems of Atomic Science and Technology. Series "Nuclear Physics Investigations"*. 2006, № 3, p. 100-104.
2. O.V. Bogdan, V.I. Karas', E.A. Kornilov, O.V. Manuilenko. 2.5-dimensional numerical simulation of a high-current ion linear induction accelerator // *Plasma Physics Reports.* 2008, v. 34, № 8, p. 667-677.
3. V.I. Karas', O.V. Manuilenko, V.P. Tarakanov, O.V. Federovskaya. Acceleration and stability of a high-current ion beam in induction fields // *Plasma Physics Reports.* 2013, v. 39, № 3, p. 209-225.
4. V.I. Karas', E.A. Kornilov, O.V. Manuilenko, et al. Transportation of high-current ion and electron beams in the accelerator drift gap in the presence of an additional electron background // *Plasma Physics Reports.* 2015, v. 41, № 12, p. 1028-1045.
5. S.N. Dubniuk, B.V. Zajtsev. The linear accelerator for radiation structural materials // *Problems of Atomic Science and Technology. Series "Nuclear Physics Investigations"*. 2014, № 3, p. 172-176.
6. R.A. Anokhin, S.M. Dubniuk, B.V. Zajtsev, K.V. Pavlii. Irradiation technique of constructional materials on the helium ions linac // *Problems of Atomic Science and Technology. Series "Nuclear Physics Investigations"*. 2016, № 3, p. 79-83.
7. R.A. Anokhin, B.V. Zaitsev, K.V. Pavlii, et al. Experimental complex for investigation of construction materials on the helium ions linear accelerator// *Problems of Atomic Science and Technology. Series "Nuclear Physics Investigations"*. 2017, № 6, p. 167-171.
8. R.A. Anokhin, V.N. Voyevodin, S.N. Dubnyuk, et al. Methods and experimental results constructions materials irradiation of helium ions at the linear accelerator // *Problems of Atomic Science and Technology. Series "Physics of Radiation Effect and Radiation Materials Science"*. 2012, № 5, p. 123-130.
9. V.A. Bomko, A.F. Burban, I.V. Vorobyova, et al. Production of track membranes with ultrasmall pores on the Kharkov heavy ions linear accelerator MILAC // *Problems of Atomic Science and Technology. Series "Nuclear Physics Investigations"*. 2008, № 5, p. 179-183.
10. *Handbook of advanced plasma processing techniques* / Ed. by R.J. Shul, S.J. Pearton. Springer, 2000, 653 p.
11. Y. Ueda, K. Schmid, M. Balden, et al. Baseline high heat flux and plasma facing materials for fusion // *Nuclear Fusion.* 2017, v. 57, p. 092006.
12. Ch. Linsmeier, B. Unterberg, J.W. Coenen, et al. Material testing facilities and programs for plasma-facing component testing // *Nuclear Fusion.* 2017, v. 57, p. 092012.
13. V.N. Voyevodin. Structural materials of nuclear power - challenge to 21 century // *Problems of Atomic Science and Technology. Series "Physics of Radiation Effect and Radiation Materials Science"*. 2007, № 2, p. 10-22.

14. I.M. Nekluydov, G.D. Tolstolutskaya. Helium and hydrogen in structural materials // *Problems of Atomic Science and Technology. Series "Physics of Radiation Effect and Radiation Materials Science"*. 2003, № 3, p. 3-14.
15. V.A. Bomko, A.P. Kobets, Z.E. Ptukhina, S.S. Tishkin. Variant alternation phase focusing with step change of the synchronous phase // *Problems of Atomic Science and Technology. Series "Nuclear Physics Investigations"*. 2004, № 2, p. 153-154.
16. V.O. Bomko, Z.E. Ptukhina, N.G. Shulika, S.S. Tishkin. Variant of focusing by an accelerating RF field in linear ion accelerators // *Proc. RUPAC-2002*. Obninsk, 2002, v. 1, p. 227-230 (in Russian).
17. V.O. Bomko, Z.O. Ptukhina, S.S. Tishkin. Variant of the accelerating and focusing structure of the high current linear ion accelerator // *Problems of Atomic Science and Technology. Series "Nuclear Physics Investigations"*. 2006, № 2, p. 163-165.
18. R.A. Demirkhanov, Yu.V. Kursanov, V.M. Blagoveschensky. Protons source of high intensity // *Instruments and Experimental Techniques*. 1964, № 1, p. 30-33.
19. V.G. Papkovich, N.A. Khizhnyak, N.G. Shulika. Alternating phase focusing in a linear ion accelerator // *Problems of Atomic Science and Technology.* 1978, № 2, p. 51-56.
20. S.S. Tishkin. Combined focusing by RF-field for ion linac accelerators // *The Journal of Kharkiv National University. Physical Series "Nuclear, Particle, Fields"*. 2008, № 808, iss. 2(38), p. 37-46.
21. L. Lu, T. Hattori, N. Hayashizaki. Design and simulation of C^{6+} hybrid single cavity linac for cancer therapy with direct plasma scheme // *Nuclear Instruments and Methods. A*. 2012, v. 688, p. 11-21.
22. V.O. Bomko, A.F. Dyachenko, B.V. Zajtsev, et al. Inductance-capacitor system for tuning of interdigital structure of the ion linear accelerator // *Problems of Atomic Science and Technology. Series "Nuclear Physics Investigations"*. 2007, № 5, p. 180-183.
23. V.O. Bomko, A.F. Dyachenko, B.V. Zajtsev, et al. Experimental modeling of the hybrid accelerating structure of heavy ion linear accelerator // *Problems of Atomic Science and Technology. Series "Nuclear Physics Investigations"*. 2016, № 3, p. 17-20.
24. V.O. Bomko, A.F. Dyachenko, B.V. Zajtsev, et al. Regulation of level RF field in hybrid structures of heavy ions linear accelerator // *Problems of Atomic Science and Technology. Series "Nuclear Physics Investigations"*. 2016, № 3, p. 21-25.
25. V.O. Bomko, B.V. Zaitsev, J.V. Ivakhno, et al. Accelerating structure with radio-frequency quadrupole (RFQ) for the heavy ions accelerating // *Problems of Atomic Science and Technology. Series "Nuclear Physics Investigations"*. 2010, № 3, p. 26-30.
26. B.V. Zajtsev, S.S. Tishkin, N.G. Shulika. The prospects for combined high-frequence focusing usage in high-current heavy ion linacs // *Problems of Atomic Science and Technology. Series "Nuclear Physics Investigations"*. 2010, № 3, p. 85-89.
27. A.F. Dyachenko, B.V. Zaytsev, S.S. Tishkin, et al. An accelerating and focusing structure with combined RF focusing for heavy ion accelerator // *Problems of Atomic Science and Technology. Series "Nuclear Physics Investigations"*. 2014, № 3, p. 16-19.
28. R.A. Anokhin, K.V. Pavlii. Influence of interacting heavy nuclei mass asymmetry on capture cross-section in fusion reactions // *Problems of Atomic Science and Technology. Series "Nuclear Physics Investigations"*. 2013, № 3, p. 151-155.
29. R.A. Anokhin, K.V. Pavlii. Dynamic-statistical description of capture cross-section – initial stage of the fusion of heavy nuclei reaction // *Problems of Atomic Science and Technology. Series "Nuclear Physics Investigations"*. 2011, № 5, p. 16-23.

Article received 10.06.2018

РАДИАЦИОННЫЙ КОМПЛЕКС НА БАЗЕ ЛИНЕЙНОГО УСКОРИТЕЛЯ ИОНОВ ГЕЛИЯ

С.Н. Дубнюк, Р.А. Анохин, А.Ф. Дьяченко, А.Ф. Кобец, А.И. Кравченко, О.В. Мануйленко, К.В. Павлий, В.Н. Решетников, А.С. Шевченко, В.А. Сошенко, С.С. Тишкин, Б.В. Зайцев, А.В. Журавлев, В.Г. Журавлев

Приведены результаты численного моделирования и экспериментального исследования линейного ускорителя ионов гелия с выходной энергией 4 МэВ с фокусировкой ВЧ-полем. Для обеспечения радиально-фазовой устойчивости ускоряемого пучка использован вариант переменно-фазовой фокусировки с шаговым изменением синхронной фазы и нарастающей амплитудой ВЧ-поля в ускоряющих зазорах на группирующем участке ускоряюще-фокусирующего тракта ускорителя. Рассмотрены способы увеличения тока ускоряемого пучка ионов, а также плотности тока пучка на мишени.

РАДІАЦІЙНИЙ КОМПЛЕКС НА БАЗІ ЛІНІЙНОГО ПРИСКОРЮВАЧА ІОНІВ ГЕЛІЮ

С.М. Дубнюк, Р.О. Анохін, О.Ф. Дьяченко, А.П. Кобець, А.І. Кравченко, О.В. Мануйленко, К.В. Павлій, В.М. Решетніков, О.С. Шевченко, В.А. Сошенко, С.С. Тішкін, Б.В. Зайцев, О.В. Журавльов, В.Г. Журавльов

Представлено результати чисельного та експериментального дослідження лінійного прискорювача іонів гелію з вихідною енергією 4 МеВ і фокусуванням ВЧ-полем. Для забезпечення радіально-фазової стійкості прискореного пучка використано варіант змінно-фазового фокусування з покроковою зміною синхронної фази і наростаючою амплітудою ВЧ-поля в прискорюючих зазорах на групуючій ділянці прискорюючо-фокусуючого тракту прискорювача. Розглянуто способи збільшення струму прискореного пучка іонів, а також щільності струму пучка на мішені.